

Agentar-Fin-OCR

Siyi Qian* Xiongfei Bai* Bingtao Fu Yichen Lu Gaoyang Zhang Xudong Yang
Peng Zhang[†]

Ant Group

{siyi.qsy, baixiongfei.bxf, biaotao.bf, luyichen.lyc, zgy528076, jiegang.yxd,
minghua.zp}@antgroup.com

Abstract

In this paper, we propose **Agentar-Fin-OCR**, a document parsing system tailored to financial-domain documents, transforming ultra-long financial PDFs into semantically consistent, highly accurate, structured outputs with auditing-grade provenance. To address finance-specific challenges such as complex layouts, cross-page structural discontinuities, and cell-level referencing capability, **Agentar-Fin-OCR** combines (1) a Cross-page Contents Consolidation algorithm to restore continuity across pages and a Document-level Heading Hierarchy Reconstruction (DHR) module to build a globally consistent Table of Contents (TOC) tree for structure-aware retrieval, and (2) a difficulty-adaptive curriculum learning training strategy for table parsing, together with a CellBBoxRegressor module that uses structural anchor tokens to localize table cells from decoder hidden states without external detectors. Experiments demonstrate that our model shows high performance on the table parsing metrics of OmniDocBench. To enable realistic evaluation in the financial vertical, we further introduce **FinDocBench**, a benchmark that includes six financial document categories with expert-verified annotations and evaluation metrics including Table of Contents edit-distance-based similarity (TocEDS), cross-page concatenated TEDS, and Table Cell Intersection over Union (C-IoU). We evaluate a wide range of state-of-the-art models on **FinDocBench** to assess their capabilities and remaining limitations on financial documents. Overall, **Agentar-Fin-OCR** and **FinDocBench** provide a practical foundation for reliable downstream financial document applications.

*Equal contribution.

[†]Corresponding to minghua.zp@antgroup.com

1. Introduction

Document parsing [54, 21, 30, 11] extracts machine-readable data from unstructured files like PDFs. As a core component of document intelligence, it is essential for powering Retrieval-Augmented Generation (RAG) [17, 12, 15] pipelines with structured, reliable context. Although recent research has explored a variety of approaches, including pipeline-based frameworks, multi-stage systems, and Multimodal Large Language Model (MLLM) [2, 50, 3] end-to-end solutions. Although existing frameworks have already achieved substantial results in page-level analysis, most document parsing models and benchmarks [57, 33, 31] continue to focus predominantly on treating pages as isolated entities. This narrow focus fails to capture the global logical flow and hierarchical structure of long documents, leading to semantic fractures and a loss of vital context.

In the financial and insurance domain, document parsing must satisfy much stricter business requirements, including accurate understanding of business scenarios, high-precision information extraction, and audit traceability. Unlike general documents, financial materials are characterized by their vast diversity and extreme length, ranging from A-share, Hong Kong, and US annual reports to audit reports and prospectuses that often span hundreds of pages. Despite the progress in existing methods, they have seen limited practical adoption in real financial scenarios due to their insufficient alignment with industry requirements. Financial document parsing introduces several unique challenges:

- **Layout Complexity:** Financial documents often use multi-column designs; standard parsers frequently read across columns, incorrectly merging unrelated text and destroying semantic meaning.
- **Semantic Fragmentation and Hierarchical Disconnect:** Financial documents are intrinsically governed by a rigorous, multi-level structural logic. However, physical pagination forcefully severs headers from their corresponding clauses, fragmenting this global hierarchy. When downstream applications like RAG and DocQA [26, 27] rely on isolated page-level parsing, they suffer from severe context loss.
- **Visual Reference Requirements:** Unlike general documents, financial institutions require reliable source referencing over intricate tables like financial statements, requiring every data point to be mapped back to precise page coordinates or specific table cells for visual auditing and compliance.
- **Absence of Financial Document Benchmark:** Existing document parsing benchmarks focus on general or academic contents, failing to represent the unique structural challenges and precision needs of the financial sector.

To comprehensively evaluate these capabilities under financial scenarios, we further construct **FinDocBench**, a document parsing benchmark oriented to financial vertical. FinDocBench comprises six distinct sub-categories of financial documents, accompanied by meticulously human-labeled and expert-verified annotations. As mentioned above, the data embodies the characteristics of financial documentation: extreme length, hierarchical headings, complex layouts, intricate cross-page tables and precise table cell localization. Alongside the dataset, we further introduce a corresponding evaluation pipeline to measure model capability when facing the mentioned challenges, including a new metric, **Table of Contents edit-distance-based similarity** (TocEDS), tree edit-distance-based similarity (TEDS) of concatenated cross-page tables and normalized edit distance (NED).

In summary, this work presents a financial scenario oriented document parsing system

designed to meet the strict, precise, and auditable requirements of real-world financial enterprise workflows. Our contributions are as follows:

- **Document-level Parsing.** To handle the structural complexity of financial documents, we propose a document-level content reconstruction algorithm with two core components: cross-page contents consolidation, which semantically concatenates cross-page text blocks and tables; and document-level heading hierarchy reconstruction, which reassigns heading levels across the entire document to ensure structural consistency.
- **Precision Table Parsing with Visual Reference.** To address the structural complexity of financial tables, we adopt a curriculum based difficulty adaptive sampling to ensure table parsing accuracy; and a cell-level visual reference that localizes cells via structural anchor token hidden states and regresses them into bounding boxes to enable finance-grade visual auditing for compliance-critical workflows.
- **Financial vertical document parsing benchmark: FinDocBench.** To evaluate parsing models in real-world financial scenarios, we introduce FinDocBench, covering diverse documents with quintessential financial characteristics and the corresponding evaluation pipeline.

2. Related Work

This section surveys the existing landscape of document parsing technologies, covering general-purpose OCR frameworks [8, 7, 30, 39], layout analysis models [55], table structure recognition methods [56, 37], and multimodal large language models for document understanding [41, 51]. We identify key limitations of current approaches when applied to financial scenarios: single-page processing, absence of cross-page semantic linking, and no audit traceability.

2.1. Traditional OCR Pipelines

Early approaches to document parsing primarily relied on modular pipelines, which decouple the process into text detection, recognition, and layout analysis. Traditional engines like Tesseract [36] and ABBYY FineReader [1] laid the foundation by focusing on character-level accuracy. More recently, frameworks such as PaddleOCR [8] have gained significant traction. Specifically, PaddleOCR’s PP-OCR series [10] provides a robust, lightweight pipeline for multi-language recognition, while its PP-Structure module [18] introduces sophisticated tools for layout analysis and table recovery.

Furthermore, the integration of deep learning led to the development of layout-aware models like LayoutLM (v1-v3) [48, 47, 14] and LayoutXLM [49], which utilize spatial coordinates and visual features as additional embeddings. While these models excel at identifying localized components (e.g., headers, footers, or individual table cells), they still operate within a “detect-then-recognize” paradigm. This modularity often leads to error accumulation across stages—where a minor detection flaw propagates into a semantic error. Crucially, even advanced frameworks like PaddleOCR are typically optimized for single-page processing. In financial contexts, they often fail to maintain semantic coherence when a single table spans multiple pages or when a financial term requires a cross-page definition, and they lack the intrinsic referencing capability needed to link extracted data back to its specific pixel-level origin for auditing purposes.

2.2. General Vision Language Models

The emergence of Vision Language Models (VLMs), such as commercial GPT series [2], Gemini family [38] and open-source Qwen collection [42, 50, 3], has demonstrated remarkable zero-shot capabilities in document reasoning. These models treat document images as visual inputs and leverage the linguistic power of LLMs to interpret contents. However, general VLMs are often criticized for their “hallucination” tendencies regarding numerical data [6, 19], which is a critical failure point for financial auditing. Moreover, their architectural design is usually optimized for natural scenes rather than document-specific features like small-font footnotes or complex cross-cell dependencies in tables.

2.3. OCR Specialized Vision Language Models

To bridge the gap between general vision and precise text extraction, recent research has pivoted towards OCR-specialized VLMs. Models like Donut [16] and Nougat [4] proposed an end-to-end Transformer architecture that maps document images directly to structured markups (e.g., JSON or LaTeX) without intermediate OCR steps. More recently, models such as Vary [44] and GOT-OCR [45] have enhanced the resolution and granularity of visual encoders to handle high-density text. Despite their progress, these models are predominantly designed for single-page or snippet-level processing. They lack the mechanism to handle long-form financial documents where semantic coherence must be maintained across dozens of pages.

3. Method

3.1. Overall Framework

As show in Figure 1, our framework transforms complex, unstructured financial documents into high-fidelity, machine-readable formats while maintaining a rigorous, end-to-end audit trail. To preserve semantic and structural continuity across fragmented layouts, the pipeline integrates cross-page consolidation with a Document-level Heading Hierarchy Reconstruction (DHR) module, which leverages multimodal features to reconstruct a coherent document-level heading hierarchy, serving as the document’s unified structural skeleton. For dense data extraction, we employ curriculum-based table parsing to adaptively handle structural complexity and utilize a novel “structural anchor token” mechanism to enable direct cell-level spatial grounding from decoder hidden states. By mapping extracted data units back to their original visual coordinates without auxiliary detectors, this unified approach ensures the precision, narrative integrity, and empirical referencing capability required for professional financial table auditing.

3.2. Cross-page Contents Consolidation

To ensure linguistic and structural continuity, we implement a consolidation mechanism that transforms disjointed pages into a fluid semantic content. This process employs semantic restoration logics for unstructured text and structured tables:

- **Cross-page Text Merge:** The system identifies cross-page text fragments at page boundaries, stripping away non-content elements such as headers and footers before merging the body text with the leading contents of the subsequent page to maintain syntactic and contextual integrity.
- **Cross-page Table Merge:** To ensure the structural integrity of long financial document with cross-page tables, we implement an adaptive heuristic-based splicing mechanism.

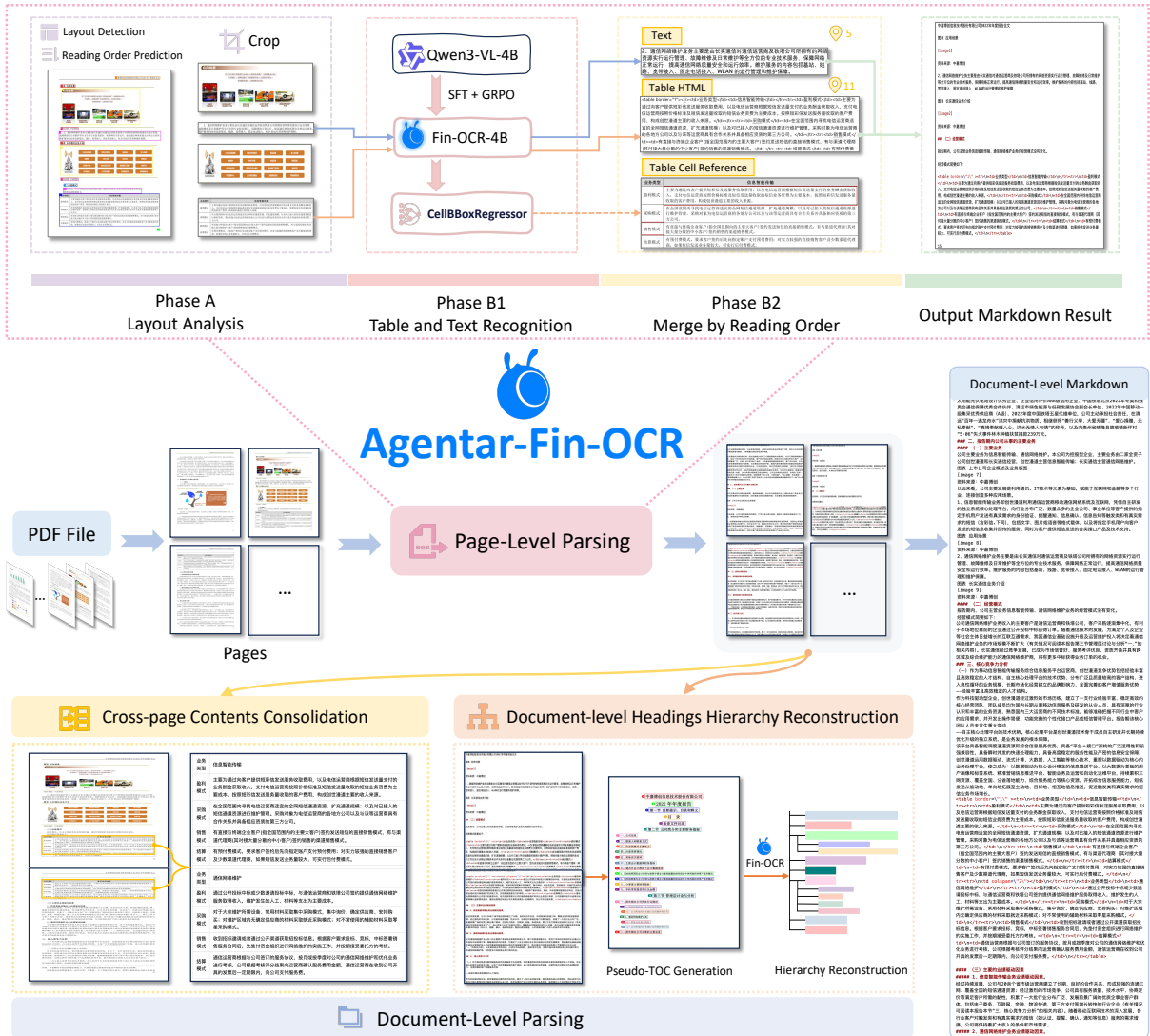


Figure 1: Agentar-Fin-OCR overall architecture.

A table fragment T_n on page n is evaluated for merging with T_{n+1} on the succeeding page based on three hierarchical criteria:

- (i) **Structural Alignment:** The column dimensions must be strictly consistent, i.e., $\text{Dim}(T_n.\text{cols}) = \text{Dim}(T_{n+1}.\text{cols})$.
- (ii) **Contextual Proximity:** To ensure physical continuity, the set of intervening semantic elements E between fragments (excluding non-content artifacts such as page headers and footers) must be empty ($E = \emptyset$). This condition confirms that the table fragments are not separated by unrelated discourse or structural interruptions.
- (iii) **Adaptive Header Splicing:** Upon satisfying (i) and (ii), the merging strategy adapts to the header content:
 - (a) **Homogeneous Splicing:** If T_{n+1} lacks a header or possesses one identical to T_n , it is treated as a seamless continuation. The redundant header is discarded, and only the `<tbody>` is appended.
 - (b) **Heterogeneous Splicing:** If T_{n+1} contains a distinct header, it indicates a categorical transition within the same structural entity. The entire fragment T_{n+1} is

merged into T_n to preserve the sub-header information. The table cases are shown in Appendix A.

The formal reconstruction procedure is detailed in Algorithm 1.

Algorithm 1 Adaptive Cross-page Table Reconstruction

Input: Sequence of table fragments $\mathcal{T} = \{T_1, T_2, \dots, T_k\}$

Output: A set of unified tables \mathcal{M}

```

1:  $\mathcal{M} \leftarrow \emptyset, T_{anchor} \leftarrow T_1$ 
2: for  $i = 2$  to  $k$  do
3:    $T_{next} \leftarrow T_i$ 
4:   // (i) & (ii) Preliminary Constraint Check
5:    $C_{align} \leftarrow (\text{Dim}(T_{anchor}.cols) = \text{Dim}(T_{next}.cols))$ 
6:    $E \leftarrow \text{GetInterveningElements}(T_{anchor}, T_{next})$ 
7:   if  $C_{align} \wedge (E = \emptyset)$  then
8:     // (iii) Adaptive Header Logic
9:     if  $\neg \text{HasHeader}(T_{next}) \vee (\text{TableHead}(T_{next}) = \text{TableHead}(T_{anchor}))$  then
10:      // Case a: Seamless Merge (Append rows only)
11:       $T_{anchor} \leftarrow \text{MergeBody}(T_{anchor}, T_{next})$ 
12:     else
13:      // Case b: Direct Full Merge (Append entire table structure)
14:       $T_{anchor} \leftarrow \text{MergeFullTable}(T_{anchor}, T_{next})$ 
15:     end if
16:   else
17:      $\mathcal{M} \leftarrow \mathcal{M} \cup \{T_{anchor}\}$ 
18:      $T_{anchor} \leftarrow T_{next}$ 
19:   end if
20: end for
21:  $\mathcal{M} \leftarrow \mathcal{M} \cup \{T_{anchor}\}$ 
22: return  $\mathcal{M}$ 

```

3.3. Document-Level Heading Hierarchy Reconstruction

Real-world financial documents often exhibit complex heading hierarchies that span dozens to hundreds of pages. This significantly undermines downstream tasks performance due to severe semantic fragmentation caused by physical pagination. To solve this problem, We propose a module for document hierarchy structure extraction, dubbed Document-level Heading Hierarchy Reconstruction (DHR). DHR transforms a sequence of isolated page-level headings into a globally consistent Table of Contents (TOC) tree, which serves as a structural abstraction for the entire document, fueling downstream tasks like RAG and document QA. The MMRAG-DocQA framework [13] validates that hierarchical indices integrating cross-page dependencies are essential for high-quality retrieval in multi-page documents. Similarly, HiChunk [24] proves that multi-level document structuring and auto-merge retrieval algorithms significantly enhance the overall reasoning precision and quality of downstream RAG systems. As we will show in Section 4.3, DHR yields substantial improvements on longer documents, while providing comparable performance on shorter documents where simpler structures are already well-captured by text alone.

In this section, we first formalize the notations and define the goal of the DHR module. We then propose its core component that achieves this TOC tree abstraction. Finally, we demonstrate

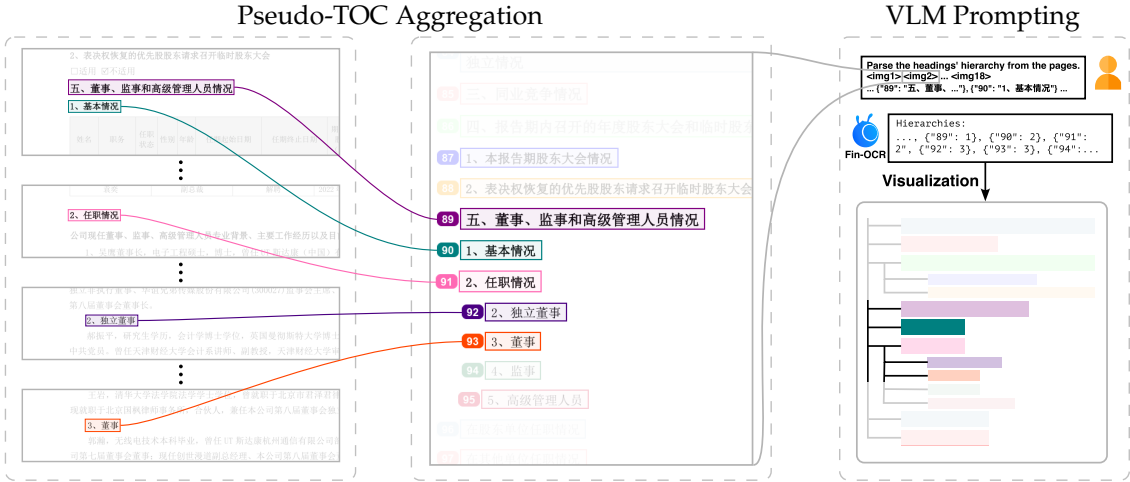


Figure 2: **Conceptual overview of the DHR pipeline.** Headings are cropped from the original documents (**left**) and aggregated into a pseudo-TOC (**middle**). The pseudo-TOC is then fed to a VLM, along with available textual information (Eq. 1), obtaining the heading hierarchy (**right**).

its impact on document intelligence applications.

3.3.1. Notations

Given a document \mathcal{D} , we denote $\mathcal{H} = \{h_1, h_2, \dots, h_n\}$ as the ordered sequence of candidate headings within \mathcal{D} . We can then characterize an entry h_i in this sequence using 4 attributes:

$$h_i = \langle \mathcal{T}_i, \mathcal{V}_i, \mathcal{S}_i, \ell_i \rangle, \text{ where} \quad (1)$$

- \mathcal{T}_i is the raw textual content of the heading.
- \mathcal{V}_i denotes the visual appearance of the header, reflecting latent typographic properties like font weight, style, and point size.
- \mathcal{S}_i is the spatial coordinates (bounding box) and page-index anchor.
- $\ell_i \in \{1, \dots, L\}$ is the heading's level (e.g., $\ell = 1$ for "Chapter", $\ell = 2$ for "Section", etc.).

Among the 4 attributes listed above, ℓ_i encodes the heading hierarchy. However, only \mathcal{T}_i , \mathcal{V}_i , and \mathcal{S}_i are available from upstream layout analysis results. We therefore propose the DHR module to recover ℓ_i , effectively reconstructing the heading hierarchy of the whole document.

3.3.2. Reconstruction Pipeline

The proposed DHR module recovers the heading hierarchy of the entire document with the help of the multi-modal reasoning ability of Fin-OCR. As illustrated in Figure 2, the module first extracts headings from the original document to form a set of images that resemble a pseudo-TOC, then it feeds the available textual results and the pseudo-TOC into Fin-OCR to reconstruct the document's heading hierarchy. We detail the process in the following.

Pseudo-TOC Aggregation. We find the layout analysis results on the original documents to provide a solid ground for accurate hierarchy reconstruction. Specifically, this includes:

- **Textual semantics from \mathcal{T}_i :** A heading h_i 's text content contextualizes itself in the whole document. When provided as additional text prompts to a VLM, it steers the VLM for more robust headings understanding (e.g., "Note 5.3" often follows "Note 5.2"), resolving potential ambiguities.
- **Visual style from \mathcal{V}_i :** In financial reports, the heading level is often indicated by consistent typography (e.g., all top-level headings share the same font size and weight, and larger-scope headings are often formatted with more prominent typesetting). In a long sequence of headings, \mathcal{V}_i provides helpful cues to mitigate level drift.
- **Spatial information from S_i :** Bounding box coordinates from the layout analysis encode the indentation pattern of headings, which provide additional cues for deeply nested heading hierarchies.

To effectively preserve these cues, we directly crop the document pages using each heading's grounded bounding box coordinates available from the previous layout analysis stage, obtaining an image crop C_i for each heading h_i (Figure 2 left). These image crops are then pasted onto an empty page-sized image, preserving their horizontal offset from the original document. By laying out all headings vertically, we can obtain a set of page-sized images, forming a *pseudo-TOC* (Figure 2 middle). Inspired by widely-used practices from the GUI agents literature [29], we also annotate the pasted heading crops with colored bounding boxes and corresponding monotonically increasing numeric labels to further boost VLM's grounding. This pseudo-TOC is later fed to the VLM and serves as the main source of heading hierarchy reconstruction.

Document-Level Heading Hierarchy Reconstruction. To finally recover the level ℓ_i of every heading from the document, we prompt the Fin-OCR model with the generated pseudo-TOC images and relevant layout analysis results (Figure 2 top-right). Specifically, we craft the text-image prompt from the following components:

- A brief, task-oriented textual instruction. E.g., "Parse the TOC pages into the following JSONL format:..."
- The text content \mathcal{T}_i of each heading extracted from the layout analysis result and the numeric label of the corresponding heading.
- The pseudo-TOC pages in order as image prompts.

The level of each heading is then recovered in the specified format, the heading hierarchy of the whole document can be easily decoded and visualized from this format (Figure 2 bottom-right).

3.4. Curriculum Learning and Reinforcement Optimization for Table Parsing

Difficulty assessment is useful not only for filtering high-quality training data but also for guiding RL optimization. Motivated by this, we collect training data from a mixture of public and in-house sources, and construct a multi-dimensional tabular annotation schema that encompasses structural attributes and stylistic formatting attributes (e.g., table line styles, blank-cell ratio, the maximum rowspan/colspan, and the distribution of rowspan/colspan values). We then build a finely annotated in-house dataset to guide targeted optimization. To identify which attributes materially affect parsing performance, we conduct a Pearson correlation analysis between each attribute $a \in \mathcal{A}$ and the model's TEDS score y on the in-house dataset:

$$\rho(a, y) = \frac{\text{cov}(a, y)}{\sigma_a \sigma_y}. \quad (2)$$

We then rank attributes by $|\rho(a, y)|$ and treat those with the largest magnitude correlations as the primary difficulty factors. We find that the following two categories of attributes are significantly negatively correlated with the final TEDS: structural complexity (e.g., the values of rowspan/colspan), and the Inference Consistency Difficulty (ICD), defined as the standard deviation of TEDS across repeated high-temperature inference runs for a given sample [30], which serves to quantify instability in structural parsing.

Based on these findings, we define a unified difficulty score $d(x)$ by combining structural complexity and ICD, and use it to organize training samples for curriculum learning:

$$d(x) = \alpha \text{Structural Complexity}(x) + \beta \text{ICD}(x). \quad (3)$$

We first perform supervised fine-tuning (SFT) on the curriculum-organized samples to establish a strong initialization. We then apply reinforcement learning with Group Relative Policy Optimization (GRPO) [35] after SFT to improve table row/column alignment. In each iteration, GRPO samples a group of responses (o_1, \dots, o_G) for a query q from the old policy $\pi_{\theta_{\text{old}}}$, and updates π_{θ} by maximizing:

$$\mathcal{L}_{\text{GRPO}}(\theta) = \mathbb{E}_{q \sim D, \{o_i\}_{i=1}^G \sim \pi_{\theta_{\text{old}}}(\cdot | q)} \left[\frac{1}{G} \sum_{i=1}^G \left(\min(r_i A_i, \text{clip}(r_i, 1 - \varepsilon, 1 + \varepsilon) A_i) - \beta D_{\text{KL}}(\pi_{\theta}(\cdot | q) \| \pi_{\text{ref}}(\cdot | q)) \right) \right], \quad r_i = \frac{\pi_{\theta}(o_i | q)}{\pi_{\theta_{\text{old}}}(o_i | q)}. \quad (4)$$

In our preliminary analysis, we observe that for structurally complex tables, the model may fail to generate row/column-aligned parses, with errors concentrated at the boundaries, in particular the last few rows and the last few columns. Beyond the TEDS reward [53], we explicitly introduce a grid-consistency signal that rewards outputs whose extracted grid signature matches the ground truth, i.e., $\mathbb{I}[g(o) = g(o^*)]$. The reward for each output o is a weighted sum of grid-consistency and TEDS:

$$R(q, o) = \lambda_1 \mathbb{I}[g(o) = g(o^*)] + \lambda_2 \text{TEDS}(\text{norm}(o), \text{norm}(o^*)), \quad (5)$$

where $g(\cdot)$ extracts the logical grid signature (expanded rowspan/colspan row-width list), and o^* is the ground-truth table. The advantage A_i is computed from group rewards using a mean-baseline within the sampled group.

To stabilize training, outputs that exceed the maximum length or violate the required table schema are assigned zero reward.

We apply an ensemble of table parsers (PaddleOCR-VL [7], Mineru2.5 [30], and HunyuanOCR [39]) for automatic pre-filtering to bootstrap an easy-stage subset with reliable supervision. Building on the difficulty score $d(x)$, we further stratify the remaining data into different difficulty levels and prioritize samples with higher difficulty for later-stage training. We continuously monitor and adjust the difficulty distribution in each sampling round to construct the advanced-stage subset, and conduct an additional training cycle on these challenging samples, thereby improving table parsing accuracy. With GRPO, the model generates better row/column-aligned parses on complex tables, especially improving alignment in the last few rows and columns. More results are given in Appendix D.

3.5. Table Parsing with Cell-Level Visual Reference

Financial document understanding in real-world business settings, such as auditing and compliance, often requires fine-grained cell-level visual references. However, most existing table

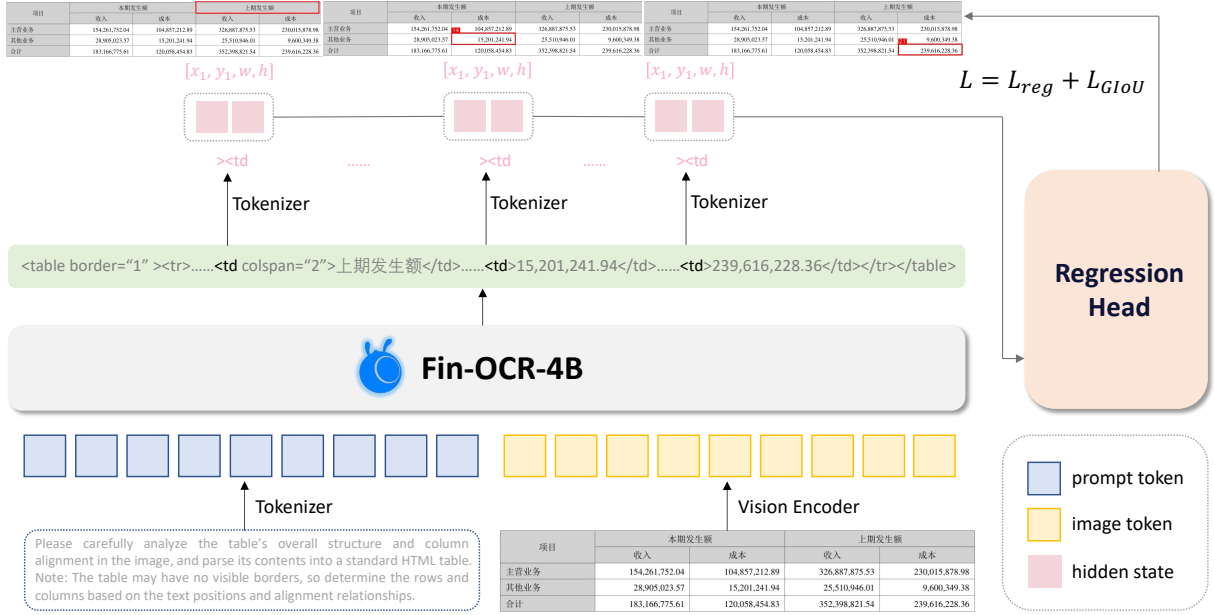


Figure 3: **Architecture of CellBoxRegressor.** CellBoxRegressor grounds each table cell by regressing its bounding box from decoder hidden states anchored at cell-start tokens.

parsing models focus on recovering the table structure (e.g., HTML) and do not provide reliable cell-level grounding that maps each predicted cell back to its precise location in the source document. While modern VLMs [3] have been explored for generic grounding tasks, a common remedy is to inject dedicated special tokens (e.g., `<bbox>`) [23] and train the model to emit coordinates. However, introducing extra special tokens increases sequence length and decoding burden, especially for tables with enormous cells, and may require non-trivial changes to the vocabulary and training recipe. To meet the cell-level grounding requirement for document tables, we propose CellBoxRegressor, as shown in Figure 3, which leverages structural anchor tokens in the HTML stream to regress bounding boxes for each cell without introducing additional special tokens.

3.5.1. Structural anchor tokens.

To enable cell-level grounding with minimal changes to the generation pipeline, we avoid introducing an extra `<bbox>` token and instead reuse cell-start anchor tokens from the HTML stream. Due to different HTML serialization styles and the tokenization, the beginning of a cell start tag `<td . . .>` can be detected in two ways: (i) a start-tag token `"<td"`; or (ii) an adjacent tag-boundary pair `"><" + "<td"` in compact HTML. We unify both cases by defining an anchor index P_k that is aligned to the start of the k -th cell start tag:

$$P_k \in \{t \mid y_t = "<td"&\} \cup \{t+1 \mid (y_t = "><" \wedge y_{t+1} = "<td")\}. \quad (6)$$

Given the HTML token sequence $Y = \{y_t\}_{t=1}^T$ and decoder hidden states $\mathbf{H} = \{\mathbf{H}_t\}_{t=1}^T$ with $\mathbf{H}_t \in \mathbb{R}^D$, we represent each cell using a fixed two-token anchor window:

$$\mathbf{s}_k = \text{Pool}(\mathbf{H}_{P_k}, \mathbf{H}_{P_k+1}) \in \mathbb{R}^{D_s}. \quad (7)$$

Here \mathbf{H}_{P_k+1} corresponds to the immediate next token after the anchor (e.g., `">"` or an attribute-related token), providing local context while keeping a consistent representation across cells.

3.5.2. Training and inference.

Training uses teacher forcing so the anchor indices P_k appear deterministically in Y , enabling one-to-one alignment between \mathbf{s}_k and \mathbf{b}_k . We optimize a box loss (e.g., ℓ_1 with optional GIoU):

$$\mathcal{L}_{\text{box}} = \frac{1}{M} \sum_{k=1}^M \|\hat{\mathbf{b}}_k - \mathbf{b}_k\|_1 (+\lambda \mathcal{L}_{\text{giou}}). \quad (8)$$

Each cell is supervised by a normalized box

$$\mathbf{b}_m = (x_1^{(m)}, y_1^{(m)}, w^{(m)}, h^{(m)}), \quad \mathbf{b}_m \in [0, 1]^4, \quad (9)$$

where (x_1, y_1) is the top-left corner and (w, h) is width/height (normalized by (W, H)). , where (x_1, y_1) is the top-left corner and (w, h) is width/height. A lightweight regressor predicts

$$\hat{\mathbf{b}}_m = g_\theta(\mathbf{s}_m), \quad g_\theta : \mathbb{R}^{D_s} \rightarrow \mathbb{R}^4, \quad \hat{\mathbf{B}} = g_\theta(\mathbf{S}) \in \mathbb{R}^{M \times 4}. \quad (10)$$

For GIoU, we convert to corners $\hat{\mathbf{b}}_m^{xyxy} = (\hat{x}_1, \hat{y}_1, \hat{x}_1 + \hat{w}, \hat{y}_1 + \hat{h})$ and clamp to $[0, 1]$.

During inference, we locate all anchor indices P_k in the generated HTML using the same rule as in training, extract \mathbf{H}_{P_k} and \mathbf{H}_{P_k+1} to form \mathbf{s}_k , and apply g_θ to obtain $\hat{\mathbf{B}}$, achieving cell-level localization without external detectors.

3.6. FinDocBench

While OmniDocBench v1.5 [31] offers comprehensive evaluations across various general document parsing sub-tasks, the financial vertical imposes following distinct requirements:

1. financial documents are characterized by **extreme length**, e.g., prospectuses and annual reports typically encompass hundreds of pages;
2. the inherent complexity of financial vertical manifests in **hierarchical headings**, prevalent **cross-page content**, **complex layouts** and **intricate tables**;
3. the auditing demands in financial scenarios necessitate **precise cell-level localization in tables**.

Existing benchmarks only sporadically address these critical features. To bridge these gaps, we introduce FinDocBench, a benchmark specifically designed to evaluate document parsing performance within the financial vertical. The overview of key features of FinDocBench is illustrated in Figure 4.

3.6.1. Data Collection

We collect publicly available financial documents via search engines and various financial consulting websites. To ensure a comprehensive distribution, the benchmark encompasses six distinct sub-categories: annual reports, research reports, audit reports, debt issuance announcements, prospectuses, and insurance documents. Their individual examples are visualized in Figure 5.

3.6.2. Data Annotation

Pre-annotation Phase: Given that state-of-the-art (SOTA) closed-source commercial pipelines and open-source multimodal models have demonstrated robust performance in single-page parsing, we adopted a ensembling pre-annotation strategy.

FinDocBench: A Financial Vertical Document Parsing Benchmark

Diverse and Specialized Document Types



Figure 4: **Overview of FinDocBench.** It contains six financial document categories and provides a comprehensive evaluation focusing on ultra-long document parsing, hierarchical heading reconstruction, and advanced table recognition.

Manual Correction Phase: Beyond refining the pre-annotations, we put more emphasis on annotations of heading hierarchies in long documents, reading order with complex financial layouts, and intricate cross-page tables. Due to the parsing challenges in financial documents, current models still struggle with such complex structural content recovery, which necessitates meticulous human intervention to ensure the accuracy of annotations.

Expert Quality Assurance: We further engaged Chartered Financial Analysts (CFAs) to perform data refinement, specifically focusing on the reading order of documents with highly complex layouts. This step ensures that the annotations in FinDocBench strictly adhere to professional financial standards and industry conventions.



Figure 5: **Typical cases of each financial document sub-category.**

Table 1: Statistics of the table recognition, layout with reading order parts in FinDocBench.

Table Recognition				Layout with Reading Order				
# of single-page tables	# of cross-page tables			Total	# of layout category	# of bboxes		
	2	3	Above			Text	Others	Total
572	425	28	19	1,044	17	18,349	20,284	38,633

3.6.3. Statistics of FinDocBench

Following the data collection and annotation phases, the dataset is partitioned into three parts: table recognition, layout with reading order and heading hierarchy reconstruction. The corresponding statistical details are summarized in Table 1 and Table 2. In the table recognition part, we intentionally emphasized cross-page tables due to their prevalence in financial scenarios. This part comprises a total of 1,044 tables, 472 of which span at least two pages. Regarding layout detection, we categorize document elements into 17 classes, with a total of 38,633 annotated instances with layout categories, reading order and contents. This part can serve as the benchmark for layout detection, reading order prediction and OCR simultaneously. For heading hierarchy reconstruction, we labeled 12,467 headings from 176 financial documents; these annotations contain the textual contents, hierarchical levels and spatial positions. The distribution of document lengths is illustrated in Figure 6, where 19.3% of the documents are long-form, exceeding 30 or even 100 pages. We also calculated the average heading depth for various document types. Specifically, annual reports, audit reports, and prospectuses all reach the average depth of 3, reflecting the inherent structural complexity of these three document categories.

Table 2: Statistics of the heading hierarchy part in FinDocBench.

Document Type	# of Docs	# of Pages	# of Headings	Avg Heading Depth
Annual Reports	27	1,328	4,331	3.32
Research Reports	67	842	1,257	1.63
Audit Reports	10	765	2,271	3.58
Debt Issuance	19	449	654	1.87
Prospectuses	25	1,409	2,850	3.52
Insurance Documents	28	286	1,104	2.10
Total	176	5,079	12,467	3.06

3.7. Evaluation of FinDocBench

Table of Contents edit-distance-based similarity (TocEDS). The heading hierarchy of a document could be represented as an ordered multi-way tree. Based on the parsing results, we segment the document into fragments by recursively splitting according to heading levels. Within each fragment, headings of the same level are sorted by their reading order to reconstruct the Table of Contents as an ordered tree. TocEDS calculates the tree edit-distance-based similarity (TEDS) between the predicted tree and the ground truth, reflecting the model capability in recognizing heading contents and hierarchical levels.

Tree edit-distance-based similarity (TEDS) of concatenated cross-page table. This evaluation

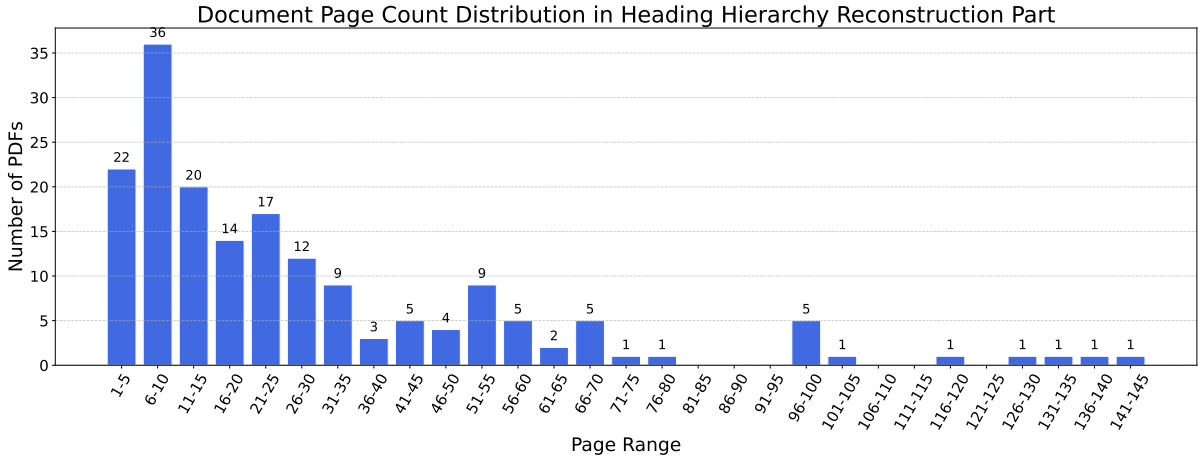


Figure 6: Page count distribution in the heading hierarchy reconstruction part.

extends TEDS to concatenated cross-page tables. It first prunes the table headers from non-initial pages and concatenates the fragments before calculating the TEDS metric against the ground truth. This metric provides an end-to-end assessment of table recognition accuracy across page boundaries.

Table Cell Intersection over Union (C-IoU). This evaluation measures cell-level localization accuracy by computing the Intersection over Union (IoU) between the predicted and ground-truth bounding boxes for each table cell. Since general-purpose VLMs and OCR systems typically do not provide explicit cell grounding outputs, we report the cell-level grounding results of our CellBBoxRegressor; as shown in Table 8, it achieves strong localization performance, indicating accurate and audit-friendly cell-level referencing capability.

4. Evaluation

4.1. OmniDocBench v1.5

To establish a comprehensive baseline for general document parsing, we first evaluate our model on OmniDocBench v1.5 [31], a widely recognized benchmark comprising 1,355 bilingual pages. Although our model is specifically tailored for financial scenarios, benchmarking on this public dataset allows for a standardized comparison with state-of-the-art methods. Given that financial documents are dominated by textual narratives and structured data, we focus our evaluation on text recognition, table parsing, and reading order. For formula recognition, we directly employ the module from PaddleOCR-VL-1.5, as formulas are less prevalent in financial reports than in scientific literature. This evaluation serves as a foundation before assessing the model on our specialized financial benchmark.

As illustrated in Table 3, our model achieves state-of-the-art results in table parsing, with a $\text{Table}^{\text{TEDS}}$ score of 92.82 and a $\text{Table}^{\text{TEDS-S}}$ score of 95.88. These results represent a significant improvement over the current leading specialized models, such as MinerU2.5 [30], DeepSeek-OCR2 [46]. Given that financial reports often contain dense and structurally intricate tables, this superior performance in TEDS metrics validates our model’s robustness in recovering complex cell relationships and hierarchical structures.

In terms of text recognition and reading order, PaddleOCR-VL-1.5 [9] maintains a slight lead, achieving the best scores of 0.035 and 0.042, respectively. Nevertheless, our model remains

Table 3: Comparison of different models on document parsing tasks. Best results are in bold.

Model Type	Methods	Overall [↑]	Overall* [↑]	Text ^{Edit} ↓	Formula ^{CDM} ↑	Table ^{TEDS} ↑	Table ^{TEDS-S} ↑	Reading Order ^{Edit} ↓
Pipeline Tools	Marker-1.8.2 [32]	71.30	68.64	0.206	76.66	57.88	71.17	0.250
	MinerU-pipeline [40]	75.51	75.00	0.209	76.55	70.90	79.11	0.225
	PP-StructureV3 [8]	86.73	87.19	0.073	85.79	81.68	89.48	0.073
General VLMs	InternVL3.5-241B [43]	82.67	80.4	0.142	87.23	75.00	81.28	0.125
	Gemini-2.5 Pro [38]	88.03	89.11	0.075	85.82	85.71	90.29	0.097
	Qwen3-VL-235B-Instruct [3]	89.15	89.66	0.069	88.14	86.21	90.55	0.068
Specialized VLMs	Dolphin [11]	74.67	78.10	0.125	67.85	68.70	77.77	0.124
	OCRFlux-3B [5]	74.82	78.23	0.193	68.03	75.75	80.23	0.202
	Mistral OCR [28]	78.83	76.82	0.164	82.84	70.03	78.04	0.144
	POINTS-Reader [22]	80.98	81.87	0.134	79.20	77.13	81.66	0.145
	olmOCR-7B [34]	81.79	79.66	0.096	86.04	68.92	74.77	0.121
	MinerU2-VLM [40]	85.56	87.87	0.078	80.95	83.54	87.66	0.086
	Nanonets-OCR-s [25]	85.59	85.42	0.093	85.90	80.14	85.57	0.108
	MonkeyOCR-pro-1.2B [21]	86.96	87.92	0.084	85.02	84.24	89.02	0.130
	MonkeyOCR-3B [21]	87.13	86.95	0.075	87.45	81.39	85.92	0.129
	dots.ocr [20]	88.41	90.99	0.048	83.22	86.78	90.62	0.053
	MonkeyOCR-pro-3B [21]	88.85	89.64	0.075	87.25	86.78	90.63	0.128
	MinerU2.5 [30]	90.67	91.76	0.047	88.46	88.22	92.38	0.044
	DeepSeek-OCR2 [46]	91.09	91.48	0.048	90.31	87.75	92.06	0.057
	PaddleOCR-VL [7]	92.86	93.70	0.035	91.22	90.89	94.76	0.043
	GLM-OCR [52]	93.94	94.15	0.043	93.51	92.60	94.84	0.043
	PaddleOCR-VL-1.5 [9]	94.50	94.63	0.035	94.21	92.76	95.79	0.042
	Ours	94.08	94.01	0.048	94.21*	92.82	95.88	0.055

The formula of Overall is calculated as: $((1 - \text{Text}^{\text{Edit}}) \times 100 + \text{Formula}^{\text{CDM}} + \text{Table}^{\text{TEDS}}) / 3$.

The formula of Overall* is calculated as: $((1 - \text{Text}^{\text{Edit}}) \times 100 + \text{Table}^{\text{TEDS}}) / 2$.

94.21*: Formula result from PaddleOCR-VL-1.5.

highly competitive, ranking within the top tier with a Text^{Edit} score of 0.048, which is on par with other high-performing models like dots.ocr and DeepSeek-OCR2 [46].

Overall, the evaluation on OmniDocBench v1.5 [31] confirms that while our model is optimized for financial scenarios, it possesses robust general document parsing capabilities. Its exceptional accuracy in table parsing provides a reliable foundation for downstream financial data analysis, where structured information is the primary focus.

4.2. Layout Detection & Reading Order Results

To evaluate the performance of our framework on complex financial documents, we conducted comparative experiments against the general-purpose PP-DocLayoutV3 baseline. Our layout analysis module is built upon the PP-DocLayout-plus-L architecture, which was further fine-tuned on a domain-specific dataset comprising insurance policies, financial reports, and bank statements. This specialized training allows the model to better capture the intricate structures (e.g., nested tables and dense multi-column text) common in financial scenarios.

Furthermore, to address reading order prediction, we implemented a 6-layer Transformer-based module that incorporates the spatial-relation modeling approach from PaddleOCR-VL. This architecture leverages self-attention mechanisms to effectively capture global dependencies among disparate layout elements. As demonstrated in Table 4, our proposed model achieves superior performance on FinDocBench, reaching a 0.873 mAP@0.5:0.95, a 0.112 improvement over PP-DocLayoutV3. More notably, our model significantly reduces the Average Relative Distance (ARD) from 0.443 to 0.075. These results validate the necessity of domain-specific fine-tuning and robust sequence modeling for maintaining logical coherence in financial document parsing. Qualitative results provided in Appendix B and Appendix C further illustrate the model’s precision in layout detection and reading order prediction.

Table 4: Financial Layout Analysis

Method	mAP ^{0.5:0.95} ↑	Reading Order (ARD) ↓
PP-DocLayoutV3	0.761	0.443
Ours	0.873	0.075

Table 5: Effect of the pseudo-TOC on document-level heading hierarchy reconstruction. Numbers in the header row (e.g., 76.50p) denote the average document length in pages.

Method	Overall (avg. pages)	Audit Reports (76.50p)	IPO Prospectuses (56.36p)	Annual Reports (49.19p)	Debt Issuance (23.63p)	Research Reports (12.57p)	Insurance Documents (10.21p)
Text-Only	0.5643	0.4322	0.7641	0.5290	0.7448	0.3808	0.3539
Text+Image (Ours)	0.6273	0.6168	0.8385	0.5893	0.7457	0.3749	0.3487

4.3. Document-level Heading Hierarchy Reconstruction

Table 5 compares our method against the text-only baseline across six financial document types, sorted by average document length. Our method achieves a higher overall TocEDS score (0.6273 vs. 0.5643), with the largest gains on longer document types: +18.5% on Audit Reports (76.50p) and +7.4% on IPO Prospectuses (56.36p). This confirms that the pseudo-TOC’s visual and spatial cues are particularly effective when heading hierarchies span many pages, where text alone struggles to resolve level ambiguities. On shorter documents, however, the two methods perform comparably, with Text-Only marginally outperforming ours on Research Reports (12.57p) and Insurance Documents (10.21p). This is expected, as shorter documents tend to have simpler and less ambiguous heading structures that are already well-captured by text alone.

4.4. Table Parsing Results

Attribute Correlation with Parsing Quality. We analyze how each attribute in our tabular label schema correlates with parsing quality. Table 6 reports the Pearson correlation between attribute values and TEDS on our in-house set. Overall, structural complexity (e.g., larger rowspan/colspan) and ICD show the strongest negative correlations with TEDS, making them effective signals for selecting high quality training data.

Quantitative results. As shown in Table 7, our approach outperforms or matches representative SOTA methods like MinerU2.5 [30] and PaddleOCR-VL-1.5 [9] across diverse benchmarks. The consistent performance gains across both public and private datasets demonstrate the efficacy of the proposed Curriculum Learning and Reinforcement Optimization strategies.

Visualization of Cell-Level Visual Reference. We visualize the predicted cell bounding boxes derived from structural anchor tokens and overlay them on the original table images. Figure 7 shows representative examples. The visualizations indicate that our CellBBoxRegressor can localize most cells accurately, including merged cells and cells at arbitrary positions, providing reliable cell-level visual references for downstream auditing and provenance tracing.

Table 6: **Pearson correlation between table attributes and TEDS.** Abbreviations: Empty Rat.=empty-cell ratio; RS=count of rowspan; CS=count of colspan; Max RS/Max CS=maximum value of rowspan/colspan; Diff. Std/Diff. Range are defined as the standard deviation/range of TEDS across repeated high-temperature inference runs for a given sample.

Attribute	Empty Rat.	Max RS	RS	Max CS	CS	Diff. Std	Diff. Range
Correlation	-0.027	-0.116	-0.174	-0.283	-0.318	-0.324	-0.332

Table 7: **TEDS comparison on different benchmarks.** * denotes the Table subset, †denotes results measured by ourselves.

Method	OmniDocBench v1.5*	PubTabNet	In-house	FinDocBench*
MinerU2.5 [30]	88.2	89.1	88.7	94.2
PaddleOCR-VL-1.5 [9]	92.8	84.6	80.7	90.5
GLM-OCR [52]†	92.6	85.2	84.4	93.0
Our	92.8	87.8	90.1	95.7

类别	期末余额		坏账准备		期初余额		坏账准备		
	金额	比例	金额	计提比例	金额	比例	金额	计提比例	
	287,225.97	0.65%	287,225.97	100.00%	287,225.97	0.65%	287,225.97	100.00%	
其中:									
按单项计提坏账准备	期末余额		坏账准备		期初余额		坏账准备		
	金额	比例	金额	计提比例	金额	比例	金额	计提比例	
	287,225.97	0.65%	287,225.97	100.00%	287,225.97	0.65%	287,225.97	100.00%	
其中:									
按组合计提坏账准备	期末余额		坏账准备		期初余额		坏账准备		
	金额	比例	金额	计提比例	金额	比例	金额	计提比例	
	43,604.84	99.35%	217,958.10	0.50%	43,386.88	27,512.43	203,886.33	0.74%	27,308.54
其中:									
按组合计提坏账准备	期末余额		坏账准备		期初余额		坏账准备		
	金额	比例	金额	计提比例	金额	比例	金额	计提比例	
	287,225.97	0.65%	287,225.97	100.00%	287,225.97	0.65%	287,225.97	100.00%	
其中:									
按组合计提坏账准备	期末余额		坏账准备		期初余额		坏账准备		
	金额	比例	金额	计提比例	金额	比例	金额	计提比例	
	43,604.84	99.35%	217,958.10	0.50%	43,386.88	27,512.43	203,886.33	0.74%	27,308.54
其中:									

类别	期末余额		坏账准备		期初余额		坏账准备			
	金额	比例	金额	计提比例	金额	比例	金额	计提比例		
按单项计提坏账准备	287,225.97	0.65%	287,225.97	100.00%	287,225.97	0.65%	287,225.97	100.00%		
其中:										
按组合计提坏账准备	43,604.84	99.35%	217,958.10	0.50%	43,386.88	27,512.43	203,886.33	0.74%	27,308.54	543.70
其中:										
按组合计提坏账准备	287,225.97	0.65%	287,225.97	100.00%	287,225.97	0.65%	287,225.97	100.00%		
其中:										
按组合计提坏账准备	43,604.84	99.35%	217,958.10	0.50%	43,386.88	27,512.43	203,886.33	0.74%	27,308.54	543.70
其中:										

项目	期初余额	本期发生额	减: 前期计入其他综合收益当期转入损益	减: 前期计入其他综合收益当期转入留存收益	税后归属于母公司	税后归属于少数股东	期末余额
	10,842,903.20	198,813.21	5,000,000.00	0	5,198,813.21	1	5,644,089.99
其他权益工具投资的公允价值变动	20	198,813.21	0	0	198,813.21	1	5,644,089.99
其他	-	-	-	-	-	-	-
分类进损益的其他综合收益	2,886,744.33	279,285.60	-	-	279,285.60	1	2,607,458.73
分类进其他综合收益	-	-	-	-	-	-	-
外币财务报表折算差额	2,886,744.33	279,285.60	-	-	279,285.60	1	2,607,458.73
合计	13,729,647.53	478,101.81	-5,000,000.00	0	9,207,748.34	2	11,251,808.72

项目	本期发生额		减: 前期计入其他综合收益当期转入损益	减: 前期计入其他综合收益当期转入留存收益	税后归属于母公司	税后归属于少数股东	期末余额
	本期发生额	本期发生额					
一、不能重分类进损益的其他综合收益	10,842,903.20	198,813.21	5,000,000.00	0	5,198,813.21	1	5,644,089.99
其他权益工具投资的公允价值变动	20	198,813.21	0	0	198,813.21	1	5,644,089.99
其他	-	-	-	-	-	-	-
二、将重分类进损益的其他综合收益	2,886,744.33	279,285.60	-	-	279,285.60	1	2,607,458.73
外币财务报表折算差额	2,886,744.33	279,285.60	-	-	279,285.60	1	2,607,458.73
合计	13,729,647.53	478,101.81	-5,000,000.00	0	9,207,748.34	2	11,251,808.72

Figure 7: **Audit visualization of cell-level referencing.** Predicted cell boxes are overlaid on the input table images.

Table 8: Cell-level grounding performance (C-IoU).

Method	IoU@0.3 \uparrow	IoU@0.5 \uparrow	IoU@0.7 \uparrow	Mean IoU \uparrow	Median IoU \uparrow
Ours	0.9765	0.9095	0.6411	0.7199	0.7555

Quantitative results. We further report quantitative localization performance using Intersection-over-Union (IoU) between the predicted and ground-truth cell bounding boxes. In FinDocBench, we collect 572 tables from financial documents as the test set. Table 8 summarizes the results on our evaluation set. The model achieves reasonable cell-level IoU, indicating that the proposed anchor-token-based regression learns a stable mapping from structural decoding states to spatial layout.

Cross-page Table Merging Results To evaluate the efficacy of the proposed cross-page merging mechanism, we curated a specialized dataset comprising 472 cross-page table instances. The experimental pipeline involved two stages: first, individual table fragments on each page were parsed using our VLM model; second, the adaptive merging algorithm described in Section 3.2 was applied to unify these fragments into integrated entities. The results demonstrate that our approach achieves an average TEDS of **0.8915** across the entire test set. This high similarity score validates the robustness of the heuristic-based splicing logic in preserving the global structural integrity of complex, cross-page tables.

5. Conclusion

In this work, we introduced Agentar-Fin-OCR, a system designed to overcome semantic fragmentation in long financial documents by shifting from page-level to document-level parsing. Our framework ensures structural continuity through cross-page consolidation and Document-level Heading Hierarchy Reconstruction, which provides a consistent structural skeleton for high-performance downstream RAG application. To meet rigorous compliance standards, we achieved audit-grade table parsing by integrating curriculum learning with a novel CellB-BoxRegressor. This mechanism leverages structural anchor tokens to enable cell-level visual referencing capability, allowing every data point to be mapped back to its source coordinates. Furthermore, we established FinDocBench, a specialized benchmark designed to evaluate the unique challenges of financial verticality, such as extreme length and complex layouts. Quantitative evaluations show that Agentar-Fin-OCR achieves state-of-the-art results in table parsing while remaining highly competitive in general document understanding. By addressing the “last-mile” precision challenge, this system provides a robust foundation for automated financial workflows, with future work focusing on multilingual expansion and deeper agentic integration to further advance automated financial intelligence.

References

- [1] ABBYY. Abby finereader pdf, 2022. URL <https://www.abbyy.com>.
- [2] Josh Achiam, Steven Adler, Sandhini Agarwal, Lama Ahmad, Ilge Akkaya, Florencia Leoni Aleman, Diogo Almeida, Janko Altenschmidt, Sam Altman, Shyamal Anadkat, et al. Gpt-4 technical report. [arXiv preprint arXiv:2303.08774](https://arxiv.org/abs/2303.08774), 2023.

- [3] Shuai Bai, Yuxuan Cai, Ruizhe Chen, Keqin Chen, Xionghui Chen, Zesen Cheng, Lianghao Deng, Wei Ding, Chang Gao, Chunjiang Ge, et al. Qwen3-vl technical report. [arXiv preprint arXiv:2511.21631](#), 2025.
- [4] Lukas Blecher, Guillem Cucurull, Thomas Scialom, and Robert Stojnic. Nougat: Neural optical understanding for academic documents. [arXiv preprint arXiv:2308.13418](#), 2023.
- [5] chatdoccom. Ocrflux, 2025. URL <https://github.com/chatdoc-com/OCRFlux>.
- [6] Zhiyu Chen, Wenhui Chen, Charese Smiley, Sameena Shah, Iana Borova, Dylan Langdon, Reema Moussa, Matt Beane, Ting-Hao Huang, Bryan Routledge, et al. Finqa: A dataset of numerical reasoning over financial data. [arXiv preprint arXiv:2109.00122](#), 2021.
- [7] Cheng Cui, Ting Sun, Suyin Liang, Tingquan Gao, Zelun Zhang, Jiaxuan Liu, Xueqing Wang, Changda Zhou, Hongen Liu, Manhui Lin, et al. Paddleocr-vl: Boosting multilingual document parsing via a 0.9 b ultra-compact vision-language model. [arXiv preprint arXiv:2510.14528](#), 2025.
- [8] Cheng Cui, Ting Sun, Manhui Lin, Tingquan Gao, Yubo Zhang, Jiaxuan Liu, Xueqing Wang, Zelun Zhang, Changda Zhou, Hongen Liu, et al. Paddleocr 3.0 technical report. [arXiv preprint arXiv:2507.05595](#), 2025.
- [9] Cheng Cui, Ting Sun, Suyin Liang, Tingquan Gao, Zelun Zhang, Jiaxuan Liu, Xueqing Wang, Changda Zhou, Hongen Liu, Manhui Lin, et al. Paddleocr-vl-1.5: Towards a multi-task 0.9 b vlm for robust in-the-wild document parsing. [arXiv preprint arXiv:2601.21957](#), 2026.
- [10] Yuning Du, Chenxia Li, Ruoyu Guo, Xiaoting Yin, Weiwei Liu, Jun Zhou, Yifan Bai, Zilin Yu, Yehua Yang, Qingqing Dang, et al. Pp-ocr: A practical ultra lightweight ocr system. [arXiv preprint arXiv:2009.09941](#), 2020.
- [11] Hao Feng, Shu Wei, Xiang Fei, Wei Shi, Yingdong Han, Lei Liao, Jinghui Lu, Binghong Wu, Qi Liu, Chunhui Lin, et al. Dolphin: Document image parsing via heterogeneous anchor prompting. In [Findings of the Association for Computational Linguistics: ACL 2025](#), pages 21919–21936, 2025.
- [12] Yunfan Gao, Yun Xiong, Xinyu Gao, Kangxiang Jia, Jinliu Pan, Yuxi Bi, Yixin Dai, Jiawei Sun, Haofen Wang, Haofen Wang, et al. Retrieval-augmented generation for large language models: A survey. [arXiv preprint arXiv:2312.10997](#), 2(1):32, 2023.
- [13] Ziyu Gong, Yihua Huang, and Chengcheng Mai. Mmrag-docqa: A multi-modal retrieval-augmented generation method for document question-answering with hierarchical index and multi-granularity retrieval. [arXiv e-prints](#), pages arXiv-2508, 2025.
- [14] Yupan Huang, Tengchao Lv, Lei Cui, Yutong Lu, and Furu Wei. Layoutlmv3: Pre-training for document ai with unified text and image masking. In [Proceedings of the 30th ACM international conference on multimedia](#), pages 4083–4091, 2022.
- [15] Zhengbao Jiang, Frank F Xu, Luyu Gao, Zhiqing Sun, Qian Liu, Jane Dwivedi-Yu, Yiming Yang, Jamie Callan, and Graham Neubig. Active retrieval augmented generation. In [Proceedings of the 2023 conference on empirical methods in natural language processing](#), pages 7969–7992, 2023.

- [16] Geewook Kim, Teakgyu Hong, Moonbin Yim, JeongYeon Nam, Jinyoung Park, Jinyeong Yim, Wonseok Hwang, Sangdoon Yun, Dongyoon Han, and Seunghyun Park. Ocr-free document understanding transformer. In European Conference on Computer Vision, pages 498–517. Springer, 2022.
- [17] Patrick Lewis, Ethan Perez, Aleksandra Piktus, Fabio Petroni, Vladimir Karpukhin, Naman Goyal, Heinrich Küttler, Mike Lewis, Wen-tau Yih, Tim Rocktäschel, et al. Retrieval-augmented generation for knowledge-intensive nlp tasks. Advances in neural information processing systems, 33:9459–9474, 2020.
- [18] Chenxia Li, Ruoyu Guo, Jun Zhou, Mengtao An, Yuning Du, Lingfeng Zhu, Yi Liu, Xiaoguang Hu, and Dianhai Yu. Pp-structurev2: A stronger document analysis system. arXiv preprint arXiv:2210.05391, 2022.
- [19] Yifan Li, Yifan Du, Kun Zhou, Jinpeng Wang, Wayne Xin Zhao, and Ji-Rong Wen. Evaluating object hallucination in large vision-language models. In Proceedings of the 2023 conference on empirical methods in natural language processing, pages 292–305, 2023.
- [20] Yumeng Li, Guang Yang, Hao Liu, Bowen Wang, and Colin Zhang. dots. ocr: Multilingual document layout parsing in a single vision-language model. arXiv preprint arXiv:2512.02498, 2025.
- [21] Zhang Li, Yuliang Liu, Qiang Liu, Zhiyin Ma, Ziyang Zhang, Shuo Zhang, Zidun Guo, Jiarui Zhang, Xinyu Wang, and Xiang Bai. Monkeyocr: Document parsing with a structure-recognition-relation triplet paradigm. arXiv preprint arXiv:2506.05218, 2025.
- [22] Yuan Liu, Zhongyin Zhao, Le Tian, Haicheng Wang, Xubing Ye, Yangxiu You, Zilin Yu, Chuhan Wu, Zhou Xiao, Yang Yu, et al. Points-reader: Distillation-free adaptation of vision-language models for document conversion. In Proceedings of the 2025 Conference on Empirical Methods in Natural Language Processing, pages 1576–1601, 2025.
- [23] Jinghui Lu, Haiyang Yu, Yanjie Wang, Yongjie Ye, Jingqun Tang, Ziwei Yang, Binghong Wu, Qi Liu, Hao Feng, Han Wang, et al. A bounding box is worth one token-interleaving layout and text in a large language model for document understanding. In Findings of the Association for Computational Linguistics: ACL 2025, pages 7252–7273, 2025.
- [24] Wensheng Lu, Keyu Chen, Ruizhi Qiao, and Xing Sun. Hichunk: Evaluating and enhancing retrieval-augmented generation with hierarchical chunking. arXiv preprint arXiv:2509.11552, 2025.
- [25] Souvik Mandal, Ashish Talewar, Paras Ahuja, and Prathamesh Juvatkar. Nanonets-ocr-s: A model for transforming documents into structured markdown with intelligent content recognition and semantic tagging, 2025.
- [26] Minesh Mathew, Dimosthenis Karatzas, and CV Jawahar. Docvqa: A dataset for vqa on document images. In Proceedings of the IEEE/CVF winter conference on applications of computer vision, pages 2200–2209, 2021.
- [27] Minesh Mathew, Viraj Bagal, Rubèn Tito, Dimosthenis Karatzas, Ernest Valveny, and CV Jawahar. Infographicvqa. In Proceedings of the IEEE/CVF Winter Conference on Applications of Computer Vision, pages 1697–1706, 2022.
- [28] Mistral AI. Mistral ocr, 2025. URL <https://mistral.ai/news/mistral-ocr>.

- [29] Magnus Müller and Gregor Žunič. Browser use: Enable ai to control your browser, 2024. URL <https://github.com/browser-use/browser-use>.
- [30] Junbo Niu, Zheng Liu, Zhuangcheng Gu, Bin Wang, Linke Ouyang, Zhiyuan Zhao, Tao Chu, Tianyao He, Fan Wu, Qintong Zhang, et al. Mineru2. 5: A decoupled vision-language model for efficient high-resolution document parsing. arXiv preprint arXiv:2509.22186, 2025.
- [31] Linke Ouyang, Yuan Qu, Hongbin Zhou, Jiawei Zhu, Rui Zhang, Qunshu Lin, Bin Wang, Zhiyuan Zhao, Man Jiang, Xiaomeng Zhao, et al. Omnidocbench: Benchmarking diverse pdf document parsing with comprehensive annotations. In Proceedings of the IEEE/CVF Conference on Computer Vision and Pattern Recognition, pages 24838–24848, 2025.
- [32] Vik Paruchuri. Marker, 2025. URL <https://github.com/datalab-to/marker>.
- [33] Birgit Pfitzmann, Christoph Auer, Michele Dolfi, Ahmed S Nassar, and Peter Staar. Doclaynet: A large human-annotated dataset for document-layout segmentation. In Proceedings of the 28th ACM SIGKDD conference on knowledge discovery and data mining, pages 3743–3751, 2022.
- [34] Jake Poznanski, Aman Rangapur, Jon Borchardt, Jason Dunkelberger, Regan Huff, Daniel Lin, Christopher Wilhelm, Kyle Lo, and Luca Soldaini. olmocr: Unlocking trillions of tokens in pdfs with vision language models. arXiv preprint arXiv:2502.18443, 2025.
- [35] Zhihong Shao, Peiyi Wang, Qihao Zhu, Runxin Xu, Junxiao Song, Xiao Bi, Haowei Zhang, Mingchuan Zhang, YK Li, Yang Wu, et al. Deepseekmath: Pushing the limits of mathematical reasoning in open language models. arXiv preprint arXiv:2402.03300, 2024.
- [36] Ray Smith. An overview of the tesseract ocr engine. In Ninth international conference on document analysis and recognition (ICDAR 2007), volume 2, pages 629–633. IEEE, 2007.
- [37] Brandon Smock, Rohith Pesala, and Robin Abraham. Pubtables-1m: Towards comprehensive table extraction from unstructured documents. In Proceedings of the IEEE/CVF Conference on Computer Vision and Pattern Recognition, pages 4634–4642, 2022.
- [38] Gemini Team, Rohan Anil, Sebastian Borgeaud, Jean-Baptiste Alayrac, Jiahui Yu, Radu Soricut, Johan Schalkwyk, Andrew M Dai, Anja Hauth, Katie Millican, et al. Gemini: a family of highly capable multimodal models. arXiv preprint arXiv:2312.11805, 2023.
- [39] Hunyuan Vision Team, Pengyuan Lyu, Xingyu Wan, Gengluo Li, Shangpin Peng, Weinong Wang, Liang Wu, Huawen Shen, Yu Zhou, Canhui Tang, et al. Hunyuanocr technical report. arXiv preprint arXiv:2511.19575, 2025.
- [40] Bin Wang, Chao Xu, Xiaomeng Zhao, Linke Ouyang, Fan Wu, Zhiyuan Zhao, Rui Xu, Kaiwen Liu, Yuan Qu, Fukai Shang, et al. Mineru: An open-source solution for precise document content extraction. arXiv preprint arXiv:2409.18839, 2024.
- [41] Dongsheng Wang, Natraj Raman, Mathieu Sibue, Zhiqiang Ma, Petr Babkin, Simerjot Kaur, Yulong Pei, Armineh Nourbakhsh, and Xiaomo Liu. Docllm: A layout-aware generative language model for multimodal document understanding. In Proceedings of the 62nd Annual Meeting of the Association for Computational Linguistics (Volume 1: Long Papers), pages 8529–8548, 2024.

- [42] Peng Wang, Shuai Bai, Sinan Tan, Shijie Wang, Zhihao Fan, Jinze Bai, Keqin Chen, Xuejing Liu, Jialin Wang, Wenbin Ge, et al. Qwen2-vl: Enhancing vision-language model’s perception of the world at any resolution. [arXiv preprint arXiv:2409.12191](#), 2024.
- [43] Weiyun Wang, Zhangwei Gao, Lixin Gu, Hengjun Pu, Long Cui, Xingguang Wei, Zhaoyang Liu, Linglin Jing, Shenglong Ye, Jie Shao, et al. Internvl3. 5: Advancing open-source multimodal models in versatility, reasoning, and efficiency. [arXiv preprint arXiv:2508.18265](#), 2025.
- [44] Haoran Wei, Lingyu Kong, Jinyue Chen, Liang Zhao, Zheng Ge, Jinrong Yang, Jianjian Sun, Chunrui Han, and Xiangyu Zhang. Vary: Scaling up the vision vocabulary for large vision-language model. In [European Conference on Computer Vision](#), pages 408–424. Springer, 2024.
- [45] Haoran Wei, Chenglong Liu, Jinyue Chen, Jia Wang, Lingyu Kong, Yanming Xu, Zheng Ge, Liang Zhao, Jianjian Sun, Yuang Peng, et al. General ocr theory: Towards ocr-2.0 via a unified end-to-end model. [arXiv preprint arXiv:2409.01704](#), 2024.
- [46] Haoran Wei, Yaofeng Sun, and Yukun Li. Deepseek-ocr 2: Visual causal flow. [arXiv preprint arXiv:2601.20552](#), 2026.
- [47] Yang Xu, Yiheng Xu, Tengchao Lv, Lei Cui, Furu Wei, Guoxin Wang, Yijuan Lu, Dinei Florencio, Cha Zhang, Wanxiang Che, et al. Layoutlmv2: Multi-modal pre-training for visually-rich document understanding. In [Proceedings of the 59th Annual Meeting of the Association for Computational Linguistics and the 11th International Joint Conference on Natural Language Processing \(Volume 1: Long Papers\)](#), pages 2579–2591, 2021.
- [48] Yiheng Xu, Minghao Li, Lei Cui, Shaohan Huang, Furu Wei, and Ming Zhou. Layoutlm: Pre-training of text and layout for document image understanding. In [Proceedings of the 26th ACM SIGKDD international conference on knowledge discovery & data mining](#), pages 1192–1200, 2020.
- [49] Yiheng Xu, Tengchao Lv, Lei Cui, Guoxin Wang, Yijuan Lu, Dinei Florencio, Cha Zhang, and Furu Wei. Layoutxlm: Multimodal pre-training for multilingual visually-rich document understanding. [arXiv preprint arXiv:2104.08836](#), 2021.
- [50] An Yang, Baosong Yang, Beichen Zhang, Binyuan Hui, Bo Zheng, Bowen Yu, Chengyuan Li, Dayiheng Liu, Fei Huang, Haoran Wei, Huan Lin, Jian Yang, Jianhong Tu, Jianwei Zhang, Jianxin Yang, Jiayi Yang, Jingren Zhou, Junyang Lin, Kai Dang, Keming Lu, Keqin Bao, Kexin Yang, Le Yu, Mei Li, Mingfeng Xue, Pei Zhang, Qin Zhu, Rui Men, Runji Lin, Tianhao Li, Tianyi Tang, Tingyu Xia, Xingzhang Ren, Xuancheng Ren, Yang Fan, Yang Su, Yichang Zhang, Yu Wan, Yuqiong Liu, Zeyu 2025, Zhenru Zhang, and Zihan Qiu. Qwen2.5 technical report. [arXiv preprint arXiv:2412.15115](#), 2024.
- [51] Jiabo Ye, Anwen Hu, Haiyang Xu, Qinghao Ye, Ming Yan, Yuhao Dan, Chenlin Zhao, Guohai Xu, Chenliang Li, Junfeng Tian, et al. mplug-docowl: Modularized multimodal large language model for document understanding. [arXiv preprint arXiv:2307.02499](#), 2023.
- [52] zai-org. Glm-ocr, 2026. URL <https://github.com/zai-org/GLM-OCR>.
- [53] Junyuan Zhang, Bin Wang, Qintong Zhang, Fan Wu, Zichen Wen, Jialin Lu, Junjie Shan, Ziqi Zhao, Shuya Yang, Ziling Wang, et al. Trivia: Self-supervised fine-tuning of vision-language models for table recognition. [arXiv preprint arXiv:2512.01248](#), 2025.

- [54] Qintong Zhang, Bin Wang, Victor Shea-Jay Huang, Junyuan Zhang, Zhengren Wang, Hao Liang, Conghui He, and Wentao Zhang. Document parsing unveiled: Techniques, challenges, and prospects for structured information extraction. arXiv preprint arXiv:2410.21169, 2024.
- [55] Zhiyuan Zhao, Hengrui Kang, Bin Wang, and Conghui He. Doclayout-yolo: Enhancing document layout analysis through diverse synthetic data and global-to-local adaptive perception, 2024. URL <https://arxiv.org/abs/2410.12628>.
- [56] Xu Zhong, Elaheh Shafieibavani, and Antonio Jimeno-Yepes. Image-based table recognition: data, model, and evaluation. In European Conference on Computer Vision, 2019. URL <https://api.semanticscholar.org/CorpusID:208267858>.
- [57] Xu Zhong, Jianbin Tang, and Antonio Jimeno Yepes. Publaynet: largest dataset ever for document layout analysis. In 2019 International conference on document analysis and recognition (ICDAR), pages 1015–1022. IEEE, 2019.

Appendix

A. Cross-page table cases

单位：元

	2022 年末		2022 年初		比重增减	重大变动说明
	金额	占总资产比例	金额	占总资产比例		
货币资金	345,352,483.61	22.54%	459,857,313.80	29.81%	-7.27%	主要系购买银行结构性存款及支付股权投资款所致
应收账款	45,109,715.95	2.94%	34,921,058.05	2.20%	0.68%	
投资性房地产	12,508,400.77	0.82%			0.82%	
长期股权投资	55,803,608.63	3.64%	70,606,734.45	4.58%	-0.94%	
固定资产	317,665,628.09	20.73%	143,226,355.40	9.28%	11.45%	主要系子公司湖南万兴外购办公楼达到预定可使用状态，转固定资产所致
使用权资产	19,318,314.58	1.28%	20,326,705.32	1.32%	-0.06%	

29

种类	期末数				账面价值
	账面余额		坏账准备		
	金额	比例(%)	金额	计提比例(%)	
单项计提坏账准备	2,955,950.40	99.57	2,955,950.40	100.00	-
按组合计提坏账准备	12,864.25	0.43	73.33	0.58	12,790.92
合计	2,968,814.65	100.00	2,956,023.73	99.57	12,790.92

(续上表)

第 98 页 共 108 页

万兴科技集团股份有限公司 2022 年年度报告全文

	2022 年末	2022 年初	比重增减	重大变动说明
合同负债	26,232,286.58	27,610,044.39	1.79%	-0.08%
租赁负债	11,752,546.27	8,257,764.03	0.54%	0.23%
其他流动资产	19,318,014.35	4,645,367.66	0.30%	0.96%
其他非流动金融资产	84,488,063.21	40,000,000.00	2.59%	2.92%
其他非流动资产	8,654,700.80	160,044,855.79	10.37%	-9.81%
长期应付款	51,600,000.00	103,178,595.40	6.69%	-3.32%

境外资产占比比较高
□适用 □不适用

(a)

种类	期初数				账面价值
	账面余额		坏账准备		
	金额	比例(%)	金额	计提比例(%)	
单项计提坏账准备	2,955,950.40	99.58	2,955,950.40	100.00	-
按组合计提坏账准备	12,370.00	0.42	42.06	0.34	12,327.94
合计	2,968,320.40	100.00	2,955,992.46	99.58	12,327.94

(b)

Homogeneous Splicing table

生产过程	主要生产内容			自产/外购/委外加工等工序类别
	硬件 DPI 探针设备	软件 DPI 探针设备 智能化应用系统 互联网信息安全管理系统 异常流量监测防护系统		
标准化软件模块设计开发	1、公司通过自主研发，完成标准化软件模块产品设计工作，并持续迭代优化和推出各类硬件 DPI 探针设备、软件 DPI 探针设备、智能化应用系统等标准化软件模块产品，其中包括： (1) 能源硬件设备研发、电路布局设计、FPGA 及相关电子元器件			自产（自研）

1-1-143

北京浩瀚深度信息技术股份有限公司 招股说明书（上会稿）

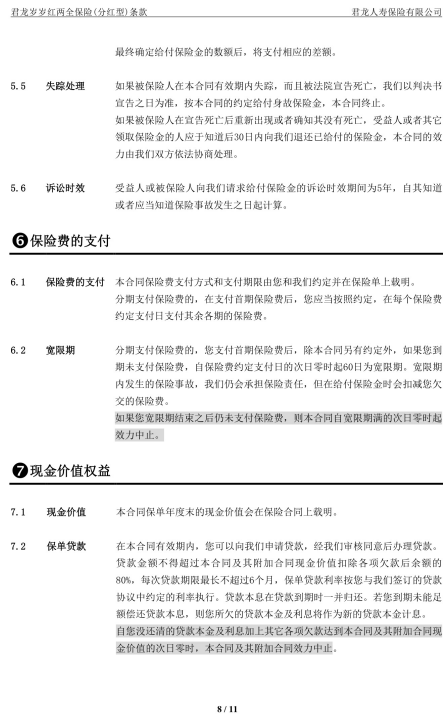
生产过程	主要生产内容		自产/外购/委外
硬件生产	定制化 PCB 裸板备货	-	基于公司设计 定制化采购
	各类电子元器件备料	-	外购
	PCB 与相关电子元器件进行焊接、贴片	-	委外加工
	PCB 模块检测及入库	-	自产
	机箱等其他配件的定制与采购	服务器、电源设备等硬件的定制与采购	基于公司设计 定制化采购
	产成品装配	-	自产
	FPGA 可编程芯片配置	软件安装	
	产成品测试、入库	产成品测试、入库	

(c)

Heterogeneous Splicing table

Figure 8: Visualization of cross-page tables.

C. Layout analysis bad cases



(a)Raw image



(b)MinerU2.5



(c)PP-DocLayoutV3



(d)Ours

Figure 10: Visualization of insurance document case.

D. GRPO Alignment Improvements

Fault Number	Detection Results								
	PCs = 8 (60% variance)			PCs = 15 (95% variance)			PCs = 19 (99% variance)		
	PCA	PCA + KFDA	PCA	PCA + KFDA	PCA	PCA + KFDA	PCA	PCA + KFDA	KFDA
1	C	B	C	A	C	B	B	B	B
2	D	B	C	A	D	A	A	A	A
3	D	B	C	A	C	B	B	B	B
4	C	A	B	A	C	A	A	A	A
5	C	A	B	A	C	A	A	A	A
6	B	B	C	B	B	B	B	B	B
7	C	B	C	A	C	B	B	B	B
8	D	B	B	A	C	A	A	A	A

Original Image

```

<table border="1"><tr><td rowspan="3">Fault Number</td><td colspan="9">Detection Results</td></tr><tr><td colspan="3">PCs = 8(60% variance)</td><td colspan="3">PCs = 15(95% variance)</td><td colspan="3">PCs = 19(99% variance)</td></tr><tr><td>PCA</td><td>PCA + KFDA</td><td>PCA</td><td>PCA + KFDA</td><td>PCA</td><td>PCA + KFDA</td><td>PCA</td><td>PCA + KFDA</td><td>PCA</td><td>PCA + KFDA</td><td>KFDA</td></tr><tr><td>1</td><td>C</td><td>B</td><td>C</td><td>A</td><td>C</td><td>B</td><td>B</td><td>B</td><td>B</td><td>B</td></tr><tr><td>2</td><td>D</td><td>B</td><td>C</td><td>A</td><td>D</td><td>A</td><td>A</td><td>A</td><td>A</td><td>A</td></tr><tr><td>3</td><td>D</td><td>B</td><td>C</td><td>A</td><td>C</td><td>B</td><td>B</td><td>B</td><td>B</td><td>B</td></tr><tr><td>4</td><td>C</td><td>A</td><td>B</td><td>A</td><td>C</td><td>A</td><td>A</td><td>A</td><td>A</td><td>A</td></tr><tr><td>5</td><td>C</td><td>A</td><td>B</td><td>A</td><td>C</td><td>A</td><td>A</td><td>A</td><td>A</td><td>A</td></tr><tr><td>6</td><td>B</td><td>B</td><td>C</td><td>B</td><td>B</td><td>B</td><td>B</td><td>B</td><td>B</td><td>B</td></tr><tr><td>7</td><td>C</td><td>B</td><td>C</td><td>A</td><td>C</td><td>B</td><td>B</td><td>B</td><td>B</td><td>B</td></tr><tr><td>8</td><td>D</td><td>B</td><td>B</td><td>A</td><td>C</td><td>A</td><td>A</td><td>A</td><td>A</td><td>A</td></tr></table>

```

GT HTML

Fault Number	Detection Results								
	PCs = 8 (60 % variance)			PCs = 15 (95 % variance)			PCs = 19 (99 % variance)		
	PCA	PCA +KFDA	PCA	PCA +KFDA	PCA	PCA +KFDA	PCA	PCA +KFDA	KFDA
1	C	B	C	A	C	B	B	B	B
2	D	B	C	A	D	A	A	A	A
3	D	B	C	A	C	B	B	B	B
4	C	A	B	A	C	A	A	A	A
5	C	A	B	A	C	A	A	A	A
6	B	B	C	B	B	B	B	B	B
7	C	B	C	A	C	B	B	B	B
8	D	B	B	A	C	A	A	A	A

Fin-OCR base

Fault Number	Detection Results								
	PCs = 8 (60 % variance)			PCs = 15 (95 % variance)			PCs = 19 (99 % variance)		
	PCA	PCA +KFDA	PCA	PCA +KFDA	PCA	PCA +KFDA	PCA	PCA +KFDA	KFDA
1	C	B	C	A	C	B	B	B	B
2	D	B	C	A	D	A	A	A	A
3	D	B	C	A	C	B	B	B	B
4	C	A	B	A	C	A	A	A	A
5	C	A	B	A	C	A	A	A	A
6	B	B	C	B	B	B	B	B	B
7	C	B	C	A	C	B	B	B	B
8	D	B	B	A	C	A	A	A	A

Fin-OCR with GRPO

Figure 11: **Qualitative comparison of table parsing results before and after GRPO.** GRPO improves row/column alignment on complex tables, with particularly noticeable gains in the last few rows and columns.